*Materials Science-Poland, 37(2), 2019, pp. 142-148*
*http://www.materialsscience.pwr.wroc.pl/*
*DOI: 10.2478/msp-2019-0033*

sciendo

# Synthesis, growth and characterization of $NaAl(SO_4)\cdot H_2O$ triangular prism single crystal for inorganic NLO application

P. SAKTHI[1], R. RAJASEKARAN[2], A. ARUN[3,*]

[1]PG & Research Deportment of Physics, Government Arts College, Thiruvannamalai-606603, Tamil Nadu, India
[2]Principal, Government Arts College, Virudhachalam-606001, Tamil Nadu, India
[3]PG & Research Department of Chemistry, Government Arts College, Thiruvannamali-606603, Tamil Nadu, India

An inorganic coordination complex of single crystal containing sodium and aluminum (SA) was grown at room temperature by slow evaporation technique. The crystal was characterized using single crystal X-ray diffraction (XRD), FT-IR, UV-Vis, SHG, SEM, EDX and TG/DTA analyses. The size of the grown crystal was around 17 mm × 15 mm × 5 mm. Both optical and SEM photographs confirmed that the crystal is transparent with smooth surface. The XRD data showed that the crystal belongs to the BCC crystal structure. The crystal shows excellent transparency in the entire region of visible light (cut-off value is 339 $cm^{-1}$). The dielectric constant as well as dielectric loss of the sample was calculated by varying frequencies at different temperatures and the presence of low dielectric loss proved that this crystal can be used for the NLO application.

Keywords: *crystal growth; X-ray diffraction; optical properties; dielectric properties*

## 1. Introduction

Nonlinear optical (NLO) materials find extensive applications in the area of laser technology, fiber optic communications, optical signal processing, optical data storage, data storage technology [1], etc. Nowadays, the novel non-linear optical materials (NLO) produced by crystal growth methods are used for the applications such as optical switching, frequency conversion and electro-optical modulation. The organic NLO materials have large nonlinear optical coefficient compared to inorganic material. However, their use is restricted due to their poor mechanical and thermal properties combined with low laser damage threshold. In contrast, the inorganic NLO materials have excellent mechanical and thermal properties. The blending between these two extremes is called a semi-organic crystal which has good mechanical properties with large damage threshold, wide transparency range, excellent nonlinear optical coefficient, low angular sensitivity [2]. To achieve the second order optical nonlinearity the desired properties of the material are transparency at required wavelengths and stable physicochemical performance [3]. The high nonlinearity enables organic crystals to double the frequency of GaAlAs diode laser for generating blue light, which is an important coherent light source. In the literature, several new classes of NLO crystals are reported that keep advantages and overcome the shortcomings of organic materials. In most of semi-organic crystals, we can find strong metal-ligand bond which permits the complex grown crystals to achieve good quality, with high nonlinearity and molecular engineering features [4]. The advantage of choosing metal complexes results in a large variety of structural modifications, high environmental stability and a much greater diversity of tunable opto-electronic properties [5, 6]. However, these semi-organic crystals have some disadvantages. The major disadvantage is the fact that two types of crystals grow simultaneously and they cannot be distinguished. The aim of this work is to synthesize an inorganic complex with high UV transparency, which can grow easily at room temperature. For this purpose, ammonium alum (as a base material) and brain solution (concentrated sodium

*E-mail: aruna2075@yahoo.co.in

chloride solution) were used and the crystals were grown at room temperature. The synthesized crystals were tested for their conductivity, morphology and UV transparency.

## 2. Experimental

### 2.1. Materials and methods

Aluminum alum and sodium chloride were received from S.D. Fine Chemical Ltd. Triple distilled water was used for the reaction to avoid any ionic impurities in the crystal. Alpha Bruker FT-IR spectrophotometer, employing KBr pellet method was used for recording the IR spectra. UV absorption measurements were recorded in the range of 200 nm to 1100 nm using LABINDIA model UV 320 instrument. Thermal analysis of the sample was carried out using a Mettler 3000 thermal analyzer operating at the heating rate of 10 °C/min in the air. The powder X-ray diffraction pattern was recorded on SA crystals crushed into fine powder using a Rigaku Minifix II-C diffractometer with CuK$\alpha$ ($\lambda = 1.5418$A Å) radiation. The sample was scanned over the range of 10° to 80°at a rate of 1°/min. Single crystal XRD analysis was carried out using Bruker AXS smart single crystal diffractometer with MoK$\alpha$ ($\lambda = 0.71069$ Å) radiation. Carl Zeiss MA15/EVO 18 instrument was used for SEM analysis and in EDX analysis, Oxford Instruments with an Aztec energy analyzer was employed. The dielectric constant of SA crystals was measured at low frequency using the LCZ meter (Model-Chen Hua 1061). The microwave benches operating at X-band and K-band were used for the dielectric studies of SA crystals. The powder SHG conversion efficiency of SA crystal was studied using Nd:YAG laser with a wavelength of 1064 nm. KDP crystal was taken as the reference to determine the conversion efficiency.

### 2.2. Synthesis of SA crystal

Aluminum alum (1 mol) and sodium chloride (1 mol) were dissolved in 500 mL of triple distilled water in an 1 liter round bottom flask fitted with nitrogen inlet and mechanical stirrer. The content of the flask was heated at 150 °C for a period of 2 h. When the solution became viscous, the heating was stopped and the content was cooled to room temperature without any disturbance. After 24 hours, the crystals were filtered in a sintered crucible and dried in air. The obtained crystals with trigonal prismatic shape were transparent.

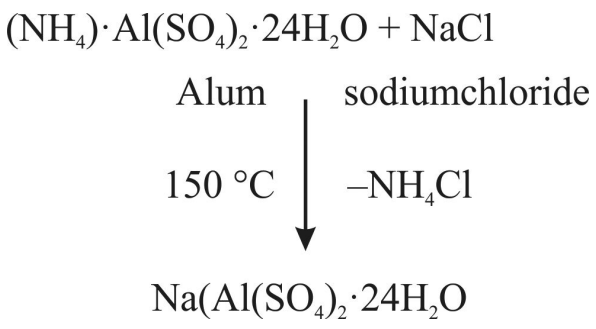


Scheme 1. Synthetic route of SA crystal.

### 2.3. Single crystal growth by slow evaporation method

The single crystal was grown by slow evaporation method. About 5 g of the SA crystal were dissolved in 50 mL of triple distilled water and stirred thoroughly. The solution was then filtered through G4 sintered crucible. The filtrate was transferred into a beaker which was kept for 15 days without any external disturbances. The SA crystals were formed in a trigonal prismatic shape.

## 3. Results and discussion

The SA crystal was synthesized using two-step method. In the first step, the crude SA crystals were prepared using high temperature reaction between the ammonium alum and the brain solution. The basic idea of the first reaction was to remove $NH_3$ molecules from the ammonium alum and introduce Na into its lattice. The completion of the reaction was confirmed by the absence of ammonium in the reaction mixture. After a required period of time, a small aliquot was taken out from the reaction mixture and tested for the presence of ammonia using Nessler's reagent. Due to the absence of reddish brown color of the reagent, it was confirmed that the sodium ion completely replaced

the ammonium in the lattice structure. Further, the gas evolving during the reaction process was tested for ammonium presence using a glass rod dipped in the concentrated hydrochloride and confirmed the presence of ammonia. The crude crystals were filtered out from the flask and large crystals were further grown by the slow evaporation technique which was described in the experimental section.

### 3.1. Optical image of SA crystal

The optical photograph of an SA crystal is shown in Fig. 1. It is seen that the grown structure is transparent with the size 17 mm × 15 mm × 5 mm.

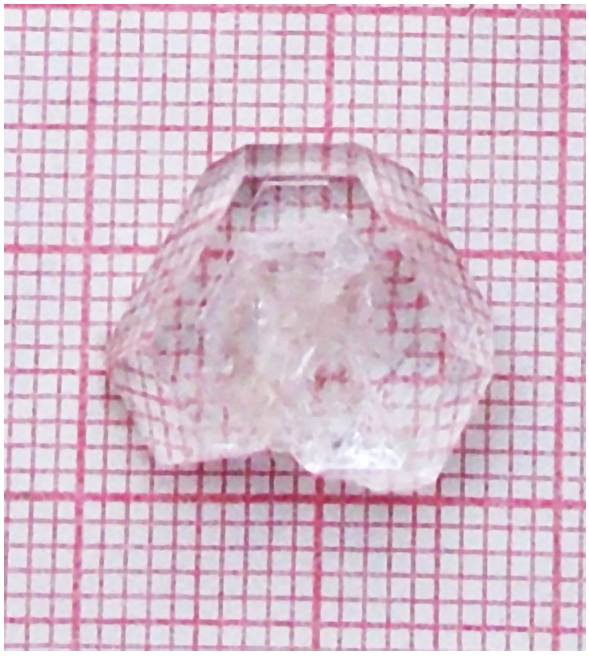

Fig. 1. Optical photograph of a grown SA crystal.

### 3.2. SEM analysis

A SEM picture of the synthesized SA crystal is shown in Fig. 2. The picture shows that the crystal is of a needle shape with defined planes and smooth surface. However, the presence of dips and cracks is also seen on the crystals surface. Thus, the SEM analysis indicates that the SA crystals possess relatively smooth surfaces and are free from major defects.

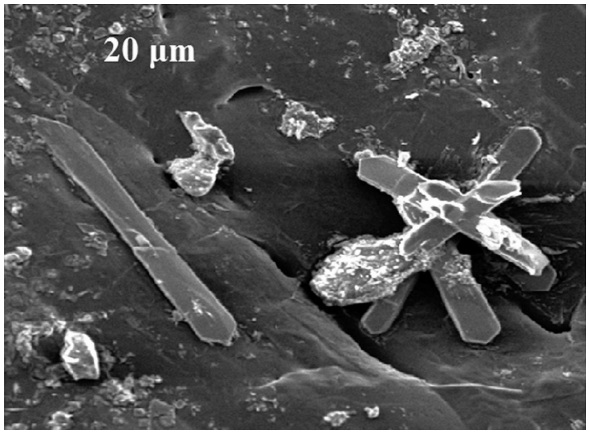


Fig. 2. SEM photograph of a crude SA crystal.

### 3.3. EDX analysis

An EDX spectrum of a SA crystal having the peaks attributed to O, Na, Al and S is shown in Fig. 3. The inset presented in Fig. 3 shows the percentage composition of the elements present in the SA crystal. These data confirm that the crystal is in highly hydrated form leading to a high percentage of oxygen molecules. The absence of peaks characteristic of nitrogen and chloride in the EDX picture confirms that the $NH_4$ and chloride ions present in the reactants were completely removed like an ammonium chloride from the reaction mixture. The elements (in atomic and weight percentages) present in the crystal are given in the Table 1.

Table 1. EDX analysis of SA crystal.

| Elements | wt.% | at.% (stoichiometry value) |
|---|---|---|
| O | 65.62 | 78.36 |
| Na | 0.55 | 0.48 |
| Al | 9.49 | 6.72 |
| S | 23.67 | 14.10 |

### 3.4. FT-IR analysis

A FT-IR spectrum of the SA crystal is presented in Fig. 4 and the data are presented in Table 2. The appearance of the broad peak at 3316 $cm^{-1}$ is due to the presence of OH stretching of water molecules which confirms that the crystal is in hydrated form. The presence of the peak at 1615 $cm^{-1}$

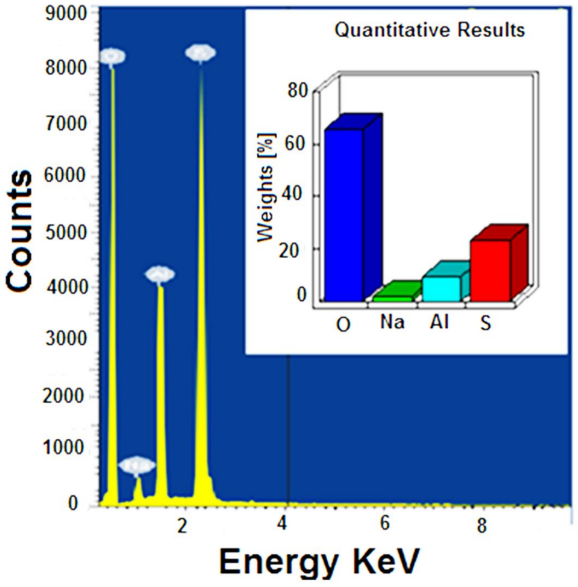


Fig. 3. EDX analysis of SA crystal.

confirms that the water molecule which is present in the complex is associated with the metal atom and can be represented as M–$OH_2$. The presence of $SO_2$ is confirmed by the presence of stretching frequencies at 1071 $cm^{-1}$, 912 $cm^{-1}$ and 615 $cm^{-1}$. These data confirm the formation of desired product which has been presented in Scheme 1.

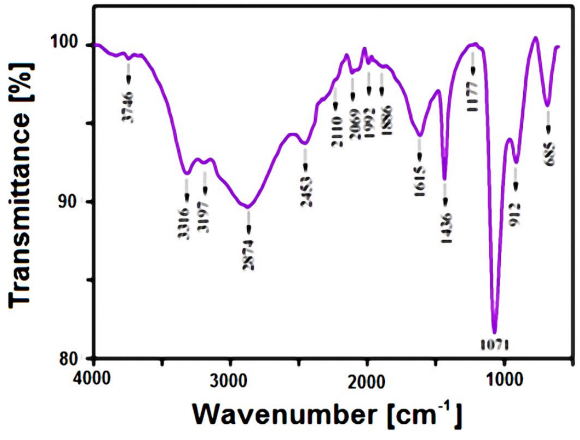


Fig. 4. FT-IR spectrum of the SA crystal.

## 3.5. UV-Vis absorbance analysis

The optical absorption spectrum of an SA single crystal, recorded in the range of 200 nm to 1100 nm, is shown in Fig. 5. It is observed from

Table 2. FT-IR spectral assignments for SA crystal.

| Wave number [$cm^{-1}$] | Assignments |
|---|---|
| 3316 | O–H and N–H stretching |
| 2874 | C–H symmetric stretching |
| 1615 | M–$OH_2$ stretching vibrations |
| 1436 | $NH_2$ stretching vibrations |
| 1071, 912, 685 | $SO_2$ stretching vibrations |

the spectrum that the SA crystal has a large transmission window lying in the range of 339 nm to 985 nm without any absorption peak. The UV cut-off wavelength of the crystal occurs at 339 nm and is closely related to the reported literature value of 345 nm for CTS crystal [7]. From this analysis, it can be concluded that the UV cut-off wavelength of the SA crystal is low with the band gap energy of Eg = 3.6 eV and 3.5 eV. It means that this crystal due to the presence of the transmission window in the whole visible region can be a good candidate for NLO applications.

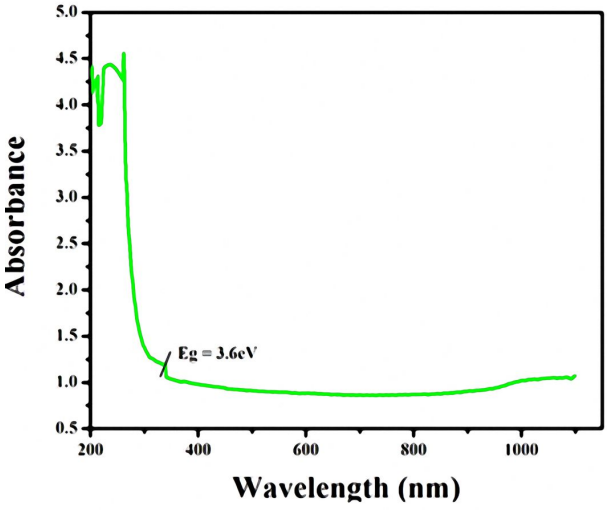


Fig. 5. Absorption spectrum of SA crystal.

## 3.6. X-ray diffraction studies.

Single crystal X-ray diffraction analysis revealed that the grown SA crystal belongs to a cubic structure with a space group of Pa3. The lattice parameters were found to be a = b = c = 12.33 Å; $\alpha = \beta = \gamma = 90°$, with the unit cell volume

V = 1877Å$^3$. The SA crystal was further subjected to powder X-ray diffraction analysis using Rigaku Minifix II-C, CuK$\alpha$ radiation of wavelength 1.5406 Å and the intensity data were recorded by continuous scanning in the range of 10° to 80° with a step size of 0.02° and step time 8 s; the corresponding graph is shown in Fig. 6. Due to the change in the cell volume parameter, the intensity of the (1 2 3) and (2 2 0) planes is very high which corresponds to JCPDS Card No. 83-1516. The single crystal XRD and powder XRD data further confirm the presence of desired crystal. The lattice parameter obtained from the single crystal XRD is exactly matched to the value of JCPDS Card No. 83-1516 which corresponds to the cubic structure. However, a small difference from the reported JCPDS value is due to the cell volume parameters. The cell volume parameter of SA is slightly higher than the reported value of hydroxyl ammonium aluminium sulphate hydrate (JCPDS Card No. 83-1516). Thus, the XRD pattern further confirms that sodium has effectively replaced ammonium in the lattice.

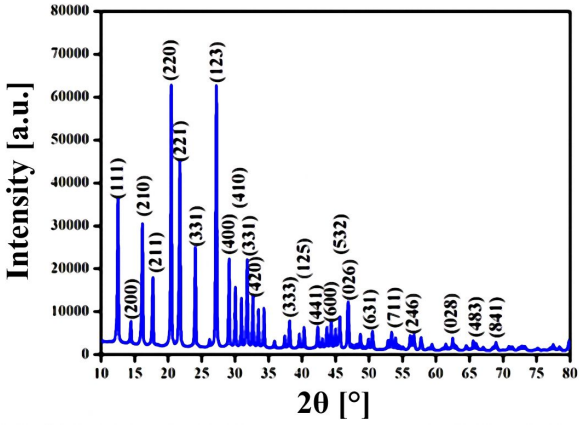


Fig. 6. PXRD pattern of SA crystal.

## 3.7. TGA and DTA analysis

The decomposition pattern of the crystal is presented in Scheme 2. Fig. 7 shows the TG/DTA curves of the SA crystal. The TGA graph shows that the SA crystal undergoes 3-stage decomposing which is confirmed by the three endothermic peaks at 300 °C, 520 °C and 750 °C, respectively. The weight loss began around 100 °C and ended at around 800 °C. The combined total mass loss is about 85 %. It was found that the most of the weight loss happened when the temperature was lower than 300 °C. The weight loss up to 300 °C is due to the loss associated with water present in the crystal. The second weight loss around 500 °C can be due to the removal of sulphur trioxide and some other small molecules from the crystal lattice. The third decomposition centered at 800 °C can be due to the removal of sodium and the formation of aluminum oxide from the coordination sphere [8].

$$\mathrm{Na[Al(SO_4)_2{\cdot}(H_2O)]{\cdot}H_2O} \xrightarrow[-\mathrm{H_2O}]{\text{up to 300 °C}} \mathrm{Na[Al(SO_4)_2]} \quad (1)$$

$$\mathrm{Na[Al(SO_4)_2]} \xrightarrow[-\mathrm{SO_3}]{\text{up to 500 °C}} \mathrm{Na + [Al_2(SO_4)_3]} \quad (2)$$

$$\mathrm{Na + [Al(SO_4)_2]} \xrightarrow[-\mathrm{SO_3}, -\mathrm{Na}]{\text{up to 800 °C}} \mathrm{Al_2O_3} \quad (3)$$

Scheme 2. Possible decomposition products of SA crystal.

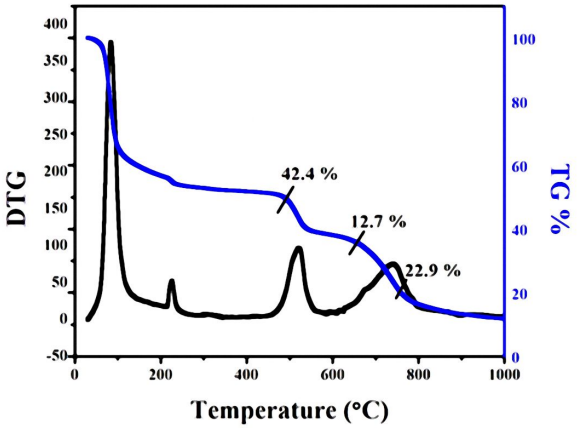


Fig. 7. TGA and DTG curves of the SA crystal.

## 3.8. Second harmonic generation (SHG) studies

The SHG efficiency of the grown crystal was measured by Kurtz and Perry powder method. The output from Nd:YAG laser ($\lambda = 1064$ nm) was used as a source to illuminate the powder form of SA which was packed in a capillary tube of a diameter 0.154 mm. Pulse energy and pulse width used for this study were 6.2 J and 10 ns, respectively.

The second harmonic signal at 523 nm was split from the fundamental frequency using an IR separator. A detector connected to the power meter was used to detect the second harmonic intensity and measure the input and output energy. The SHG efficiency of the SA crystal is comparable with the value of KDP crystal and was found to be nearly 1.2 times higher than that of KDP.

### 3.9. Dielectric studies

The dielectric properties of optical materials are connected with their electro-optic properties. A cut and polished SA crystal with dimension of 2.45 mm × 4.14 mm × 3.79 mm was used for the dielectric measurement. The variation of dielectric constant as a function of frequency (100 Hz to 5 MHz) at different temperatures is shown in Fig. 8. The dielectric constant was calculated using the formula:

$$\varepsilon_r = C_d/A \cdot \varepsilon_o \tag{1}$$

where A is the area of the sample, C is the capacitance, d is the thickness and $\epsilon_o$ is the absolute permittivity of the free space. The value of dielectric constant is high at lower frequency, then it rapidly decreases as frequency increases and at the frequency above 100 Hz, remains stable. The value of dielectric constant at low frequency was calculated as 16000 at 353 K. The decrease in dielectric constant at 100 Hz frequencies is attributed to the absence of space charge polarization near the grain boundary interface [9, 10]. The nature of the variation is similar at different temperatures. The decrease in dielectric constant at a higher frequency may be attributed to the contribution of the electronic, ionic, orientation and space charge polarizations which depend strongly on frequency. The variation of dielectric loss with frequency at different temperatures is shown in Fig. 9. The dielectric loss decreases initially with an increase in frequency and then attains a constant value of 0.25 at 100 Hz. The high dielectric loss at low frequency region may be associated with ionic mobility of the compound. The low dielectric loss at high frequency suggests that the material possesses an enhanced optical quality with lesser defects and this parameter is important for nonlinear optical applications. For materials suitable for the potential applications in NLO devices, dielectric loss must be kept as low as possible. For this reason, the synthesized SA crystal can be a potential candidate for NLO applications.

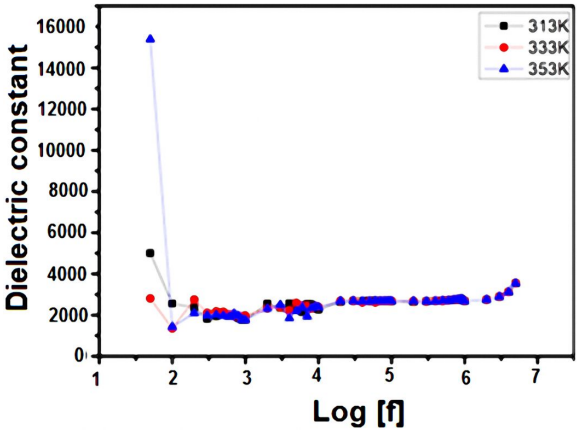


Fig. 8. Variation of dielectric constant with frequency.

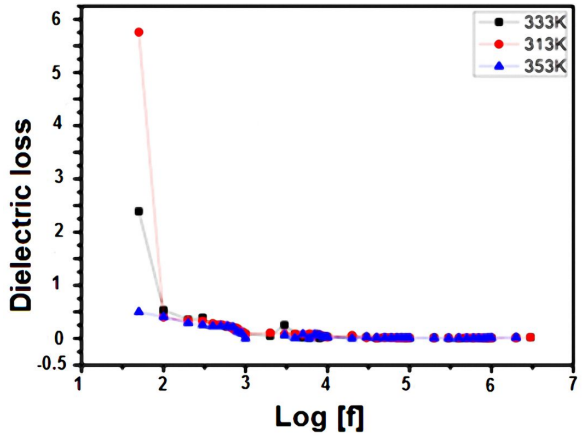


Fig. 9. Variation of dielectric loss with frequency.

## 4. Conclusions

The SA crystal was prepared by two-step process. In the first step, ammonium ion in ammonium alum was replaced by a sodium ion. In the second step, the crystal has grown using slow evaporation method. The grown crystal was about 17 mm × 15 mm × 5 mm in size with excellent

transparency in the visible region and the cut-off value of 339 nm. The IR data confirmed the formation of the desired crystal. The optical photograph and SEM photograph confirmed that the crystal has smooth surfaces and is transparent. EDX analysis was performed and the elemental composition and weight percentage present in the crystal were determined. The obtained results are consistent with the data of proposed product. The SA crystal showed three stage decomposition weight loss. The low dielectric loss of the crystal confirmed by dielectric studies implies that this material could be a potential candidate for NLO applications.

## Acknowledgements

The author thanks to the Center for Nanoscience and Crystal Growth, Anna University, Chennai, India, for Powder XRD, TGA/DTA and EDX studies.

## References

[1] RAJASEKARAN R., MOHAN KUMAR R., JAYAVEL R., RAMASAMY P., *J. Cryst. Growth*, 252 (2003), 317.

[2] ILANGO E., RAJASEKARAN R., SHANKAR K., KRISHNAN S., CHITHAMBARAM V., *Opt. Mater.*, 37 (2014), 666.

[3] RAJESH KUMAR T., JEYESEKARAN R., RAVI KUMAR S.M., VIMALA M., SAGAYARAJ P., *Appl. Sururf. Sci.*, 257 (2010), 1684.

[4] DUORONG Y., ZHENWU Z., MINGGUO, SUOYING S., MINHUA J., *J. Cryst. Growth*, 186 (1998), 240.

[5] VIJAYABHASKARAN B., C. RAMACHANDRA RAJA C., *Optik.*, 124 (2013), 1366.

[6] SELVAKUMAR S., RAVI KUMAR S.M., JOSEPH G.P., RAJARAJAN K., MADHAVAN J., S.A. RAJASEKAR S.S., SAGAYARAJ P., *Mat. Chem. Phys.*, 103 (2007), 153.

[7] KIRUBAVATHI K., SELVARAJU K., VALLUVAN R., KUMARARAMAN S., *Mater. Lett.*, 61(2007), 4173.

[8] WOJCIECHOWSKA R., WOJCIECHOWSKI W., KAMINSKI J., *J. Therm. Anal. Calorim.*, 33 (1988), 503.

[9] SELVARAJAN P., DAS B.N., GON H.B., RAO K.V., *J. Mater. Sci.*, 29 (1994), 4031.

[10] PRASAD N.V., PRASAD G., BHIMASANKARAN T., SURYANARAYANA S.V., KUMAR G.S., *Indian J. Pure Ap. Phy.*, 34 (1996), 639.

*Received 2016-05-19*
*Accepted 2018-06-22*